



# Graphene oxide as high-performance dielectric materials for capacitive pressure sensors



Shu Wan<sup>a, b</sup>, Hengchang Bi<sup>a, b</sup>, Yilong Zhou<sup>a</sup>, Xiao Xie<sup>a</sup>, Shi Su<sup>a, c</sup>, Kuibo Yin<sup>a, c</sup>, Litao Sun<sup>a, b, c, \*</sup>

<sup>a</sup> SEU-FEI Nano-Pico Center, Key Laboratory of MEMS of Ministry of Education, Collaborative Innovation Center for Micro/Nano Fabrication, Device and System, Southeast University, Nanjing 210096, PR China

<sup>b</sup> Center for Advanced Carbon Materials, Southeast University and Jiangnan Graphene Research Institute, Changzhou 213100, PR China

<sup>c</sup> Southeast University-Monash University Joint Research Institute, Suzhou 215123, PR China

## ARTICLE INFO

### Article history:

Received 22 June 2016

Received in revised form

6 December 2016

Accepted 7 December 2016

Available online 10 December 2016

## ABSTRACT

Graphene oxide (GO) foam exhibits both excellent elastic property and high relative dielectric permittivity, which is a novel building block for future wearable electronic devices. Herein we present an ultra-sensitive GO-based capacitive pressure sensor with graphene as electrodes by an efficient, low-cost fabrication strategy over large-area integration as well as patterning for recording spatial pressure distribution. The GO-based sensor can detect a subtle pressure of  $\sim 0.24$  Pa with a fast response time ( $\sim 100$  ms) and a high sensitivity ( $\sim 0.8$  kPa<sup>-1</sup>). The superior sensing properties combining with good flexibility and robustness reveal a great application potential in various fields, such as health monitoring, flexible human-computer user interfaces, and robotics, which also give a new insight for all-carbon electronics.

© 2016 Elsevier Ltd. All rights reserved.

## 1. Introduction

Recent development in electronics focuses on flexible devices for applications which involve integration with the wireless health monitoring, electronic skin, flexible sensor networks, artificial muscles, flexible human-computer interfaces, and engineered tissue constructs [1–3]. Electronic skin [4–6] has a great potential and elicits considerable attention because numerous functions of biological skin can be realized. Lots of physical variables, such as pressure [7–14], strain [15], temperature [16], humidity [17], and other parameters, can be transformed into electronic signals. A number of flexible pressure sensors have been reported recently; these sensors include those based on microstructured rubber dielectric layers capacitors [6], organic field-effect transistors [8,10,18–20], organic microstructured piezoresistors [14,21–24], carbon nanotubes [25], graphene [26,27] and graphene-coated polymer foam [28], nanowires [29], and nanoparticles [30,31]. These sensors exhibit novel sensitivity, fast response, high spatial

resolution, durability, and even self-healable ability [32,33]. In addition, by using low-modulus elastomer, several sensors with ultrahigh sensitivity in the low pressure regime ( $< 1$  kPa) have been reported in recent years [6,29,31,34,35], which have overcome the insensitive problem of sensors based on rubber thin films [18,22].

Pressure sensors based on transistors show excellent sensing properties with ultrahigh sensitivities [10,20]. However, those active devices are less power-efficient compared with passive sensors based on resistive and capacitive sensors. In addition, considering the better compatibility with wireless detection systems [36], the developments of capacitive sensors could be more valuable than resistive ones.

Capacitance variation detection has been utilized in pressure sensing and is widely investigated [6,36–44]. The effective relative dielectric permittivity of sensors, which can be varied with applied pressure, is crucial to sensitivity. Finding a novel dielectric material with a suitable structure is a possible means to improve sensitivity. Graphene oxide (GO) is a very important derivative of graphene, and it is a 2D crystal with many good mechanical, thermal, and electrical properties [45–47]. The basal plane along with the edges of GO platelets consist of distributed functional groups containing oxygen [48,49], such as hydroxyl, epoxy, and carboxyl groups (supporting information in Figs. S1–S4). These functional groups

\* Corresponding author. SEU-FEI Nano-Pico Center, Key Laboratory of MEMS of Ministry of Education, Collaborative Innovation Center for Micro/Nano Fabrication, Device and System, Southeast University, Nanjing 210096, PR China.

E-mail address: [slt@seu.edu.cn](mailto:slt@seu.edu.cn) (L. Sun).

together with structural defects strongly hinder the transfer of electrons along the GO plane. Hence, GO sheets behave like insulators, with differential conductivity values of  $1\text{--}5 \times 10^{-3}$  S/cm depending on the oxidation degree [50] and exhibit high relative dielectric permittivity (in the order of  $10^4$  within the frequency range of 0.1–70 Hz) according to a recent report [51]. Numerous studies [52–55] have proven that GO can be a feasible building block to assemble 3D ultra-light porous GO foam with good elastic property. Its novel elastic property and high relative dielectric permittivity make GO foam a good candidate as dielectric layer to fabricate highly sensitive flexible pressure sensors. Recently, graphene foam based resistive flexible pressure sensors have been reported and exhibited a great potential in flexible electronics [28]. However, there is little report about pressure sensors based on graphene oxide foam, which can be a good candidate in flexible pressure sensors as dielectric materials due to its high relative dielectric permittivity.

A simple means to fabricate a new type of flexible pressure sensor is reported in this paper. The key dielectric layer consists of thin GO foam with a low effective elastic modulus, which contributes to the high pressure sensitivity of the devices. The direct dependence on dielectric capacitance in these flexible pressure sensors enables the detection of applied pressure and causes the devices to exhibit excellent pressure sensitivity in a low-pressure regime ( $<1$  kPa). The GO-based sensor can detect a subtle pressure of  $\sim 0.24$  Pa with a fast response time ( $\sim 100$  ms) and a high sensitivity ( $\sim 0.8$  kPa $^{-1}$ ). The sensitivity is  $2 \times 10^3$  times higher than that of a flat PDMS layer [37],  $1.6 \times 10^3$  times higher than that of polyolefin foam [38],  $1.6 \times 10^2$  times higher than that of air gap [39], 4 times higher than that of a PDMS-coated layer [40], and higher than the sensitivity of a structured PDMS layer (0.55 kPa $^{-1}$ ) [6]. In addition, the sensor exhibits a rapid relaxation time ( $\ll 1$  s), good durability ( $>1000$  loading-unloading cycles and  $>1000$  flexing cycles), and the spatial resolution to locate pressure, showing great

potential in subtle pressure detecting in the low loading range.

## 2. Experimental

### 2.1. Device fabrication

The GO foam was fabricated into capacitive pressure sensors by sandwiching the foam between poly (ethyleneterephthalate) (PET) sheets with patterned, reduced GO electrodes. The as-fabricated square pressure-sensitive pad was  $1 \times 1$  cm $^2$ . The fabrication procedure is schematically shown in Fig. 1(a). Spray-coating through a stencil mask produced GO pattern lines on the PET substrate (step 1) and followed by reduction with hydriodic acid (HI) (step 2). GO solution was applied to the back side of the PET substrate with reduced GO electrodes (step 3); in this step, the density of the as-prepared GO foam can be simply modified by changing the concentration of GO solutions. The GO solution was frozen at a temperature of  $-50$  °C (step 4) for half an hour and then dried in a vacuum condition for  $\sim 12$  h to form a thin GO foam (thickness of  $\sim 300$   $\mu$ m) without any structure damage (step 5). After that, another patterned substrate was positioned (face to face) over the first one to sandwich the as-prepared thin GO foam; the two substrates were sealed with PDMS to avoid access to moisture (step 6). Fig. 1(b)–1(d) show SEM images that present detailed structure information of the press-sensitive sensor arrays. Fig. 1(b) shows the surface morphology of the reduced GO electrodes and demonstrates the uniformity and flatness of the reduced GO electrodes produced through spray-coating; the conductivity of these electrodes is  $\sim 100$  S/cm (standard four-point probe measurement at room temperature). Cross section of the electrode and PET substrate is presented in Fig. 1(c). The reduced GO electrode with a layered structure and the insulating PET are roughly separated by a red dashed line, indicating a good lamination. The porous structure of the dielectric thin GO foam is clearly shown in Fig. 1(d). The

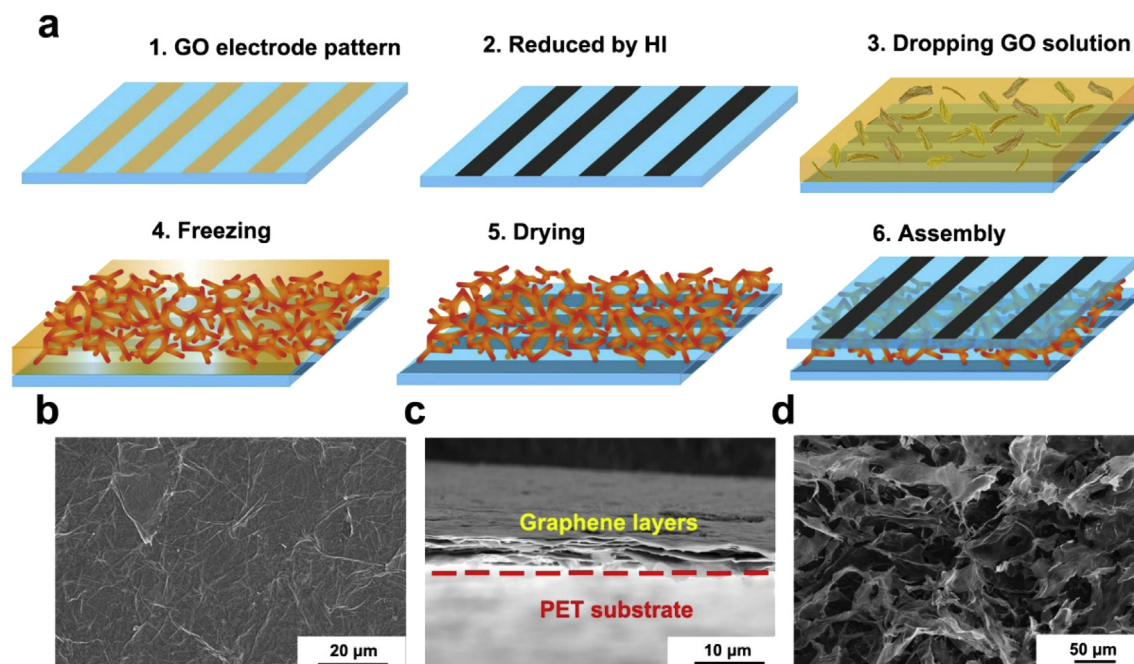


**Fig. 1.** Fabrication of prototype pressure sensor arrays. (a) Schematic of the fabrication of GO foam-based pressure sensor arrays. Spray-coating through a stencil mask produced lines of GO pattern on the PET substrate (step 1). The GO pattern was reduced by hydriodic acid (HI) (step 2). The GO solution was applied to the back side of the PET substrate with reduced GO electrodes (step 3). The GO solution was frozen at a temperature of  $-50$  °C (step 4) and then dried in a vacuum condition to form thin GO foam (thickness of  $\sim 300$   $\mu$ m) (step 5). A second patterned substrate was positioned (face to face) over the first to sandwich the as-prepared thin GO foam; the two substrates were sealed with PDMS (step 6). (b) SEM image of the surface morphology of reduced GO electrode. (c) SEM image of the cross section of the reduced GO electrode and PET substrate, which are roughly separated by a red dashed line. (d) SEM image of the thin GO foam layer. (A colour version of this figure can be viewed online.)

average pore size is about several tens of micrometers. Such pores combined with GO skeleton contribute to the elasticity of GO foam.

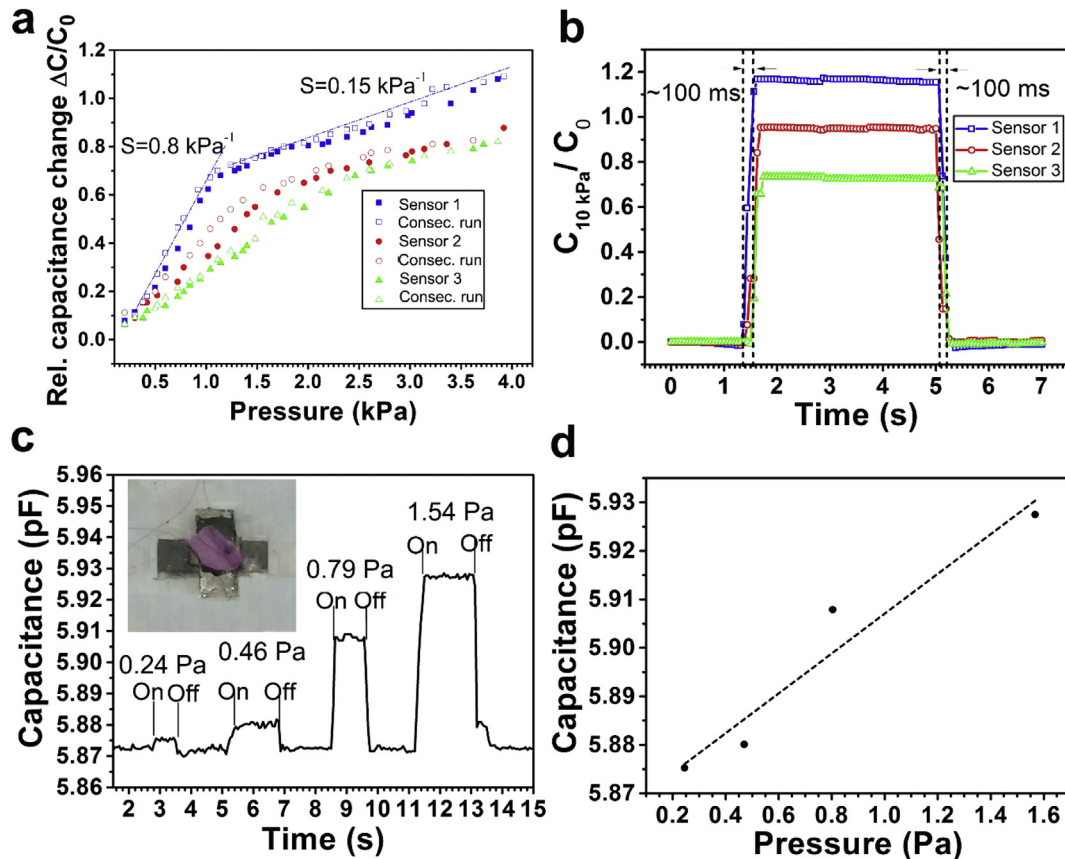
## 2.2. Pressure-sensing properties of the GO foam-based sensors

Fig. 2 shows the pressure-sensing properties of the GO foam-based sensors. A z-stage was utilized and combined with a force gauge to make a well-defined load. In Fig. 2(a), it is shown that the pressure response curve (measured twice consecutively: first run, filled symbols; second run, open symbols) of sensitivity on GO foams with different densities, namely, 1.1, 4.8, and 9.8 mg/cm<sup>3</sup> (the difference among them is clearly demonstrated by scanning electron microscopy in supporting information Fig. S5); the corresponding sensors are denoted as sensors 1, 2, and 3, respectively. The operating frequency for the testing was 1 MHz. According to the previous report [6], the pressure sensitivity  $S$  is the slope of capacitance versus pressure [6] as follows:  $S = d(\Delta C/C_0)/dp = (1/C_0) \times dC/dp$ . In this formula,  $p$  is the applied pressure;  $C$  and  $C_0$  are the corresponding capacitances with and without applied pressure. At the very low pressure regime (0–1 kPa), sensor 1 exhibited a high sensitivity of  $\sim 0.8 \text{ kPa}^{-1}$ , which is the highest among the three sensors (sensor 2:  $\sim 0.44 \text{ kPa}^{-1}$ ; sensor 3:  $\sim 0.28 \text{ kPa}^{-1}$ ), and demonstrating the ability in detecting subtle pressure. Also, the microstructure of GO foam shows little damage after 1 kPa pressure according to the SEM images in Fig. S6 (a) and (b) (supporting information). At the pressures regime above 1 kPa, the sensitivity decreased to  $\sim 0.15 \text{ kPa}^{-1}$ . The decrease in sensitivity is ascribed to the increasing elastic resistance with increasing compression

depending on the density of the GO foams (in essence, different air/GO volume ratios) [6]. The results indicate that either sensitivity or pressure range can be tunable by changing the density of the GO foams. All three sensors showed an instant response to external loading and unloading in Fig. 2 (b), and the response and relaxation times are approximately 100 ms (the resolution limit of our measurement system). Sensor 1 can detect the placement and removal of several ultra-small weights. For instance, different sizes of petals (weight: 2.5, 4.8, 8.2, and 16 mg corresponding to pressure of 0.24, 0.47, 0.8, and 1.6 Pa, respectively) was placed and removed from a thin square glass plate which covers the entire sensing area (Fig. 2 (c)). The operating frequency for the testing was set to be 1 MHz. The response to the subtle pressure was almost linear (Fig. 2(d)). The pressure detection limit of our sensors was 0.24 Pa, which is the lowest pressure detected by capacitive pressure sensors as far as we know. The high sensitivity of the GO foams can be ascribed to two main factors. First, due to the existence of air voids, GO foams shows low elastic resistance. Second, when the GO foams compressed, the air is displaced, which has a relative lower dielectric constant ( $\epsilon = 1.0$ ) compared with GO ( $\epsilon = \sim 10$ , at 1 MHz). Consequently, the capacitance increase in the GO foams attributes to both the distance reduction between the two electrode plates as well as the increase of effective dielectric constant.

## 2.3. Stability of the sensor

Sensor 2 was selected to test the stability of the proposed sensors. By loading and unloading an object that weighs 30 g



**Fig. 2.** Pressure-sensing properties of GO foam based sensors. (a) Pressure response of GO foams with different densities, namely, 1.1, 4.8, and 9.8 mg/cm<sup>3</sup> (measured twice consecutively: first run, filled symbols; second run, open symbols). The operating frequency of LCR meter was set to be 1 MHz. (b) Instant response of pressure sensors, which exhibit response and recovery times about 100ms. (c) Transient response to the placement and removal of several ultra-small weights, such as different sizes of pedals (weight: 2.5, 4.8, 8.2, and 16 mg; corresponding pressure: 0.24 Pa, 0.46 Pa, 0.79 Pa, and 1.54 Pa) in the GO foam-based sensor. Inset: a petal on the sensor. The operating frequency of LCR meter was 1 MHz. (d) Capacitive response to subtle pressures; good linearity is exhibited. (A colour version of this figure can be viewed online.)

(corresponding pressure: 3 kPa) over a thousand cycles, the test for sensor repeatability can be obtained and the result has been shown in Fig. 3 (a). In addition, the flexing durability has also been tested by bending the sensor with an angle between horizontal direction and the bending direction of  $\sim 30^\circ$  (One end was kept fixed and the other end was bent to a certain angle, Fig. S7 in supporting information) for a thousand cycles. Fig. 3 (b) exhibited the result. Minimal fluctuation was observed in both compression and bending results and the performance loss of the device was less than 1% after 1000 loading-unloading cycles, indicating no deterioration in structure. What's more, the stability could be further improved by better encapsulation. By varying the testing frequency (from 1 kHz to 1 MHz), the sensitivity of the sensor deviated little according to results shown in Fig. 3 (c) and 3 (d), which indicate that the proposed sensor can be utilized in a wide range of frequency. The

hysteresis test has also been conducted and minimal pressure hysteresis (maximum hysteresis is less than 5% at 1.4 kPa) was observed (Fig. 3 (e)). Fig. 3 (f) shows the temperature dependence of the sensor. The capacitance change increased with the temperature most likely as a result of the thermal expansion of the GO foam (capacitance is inversely proportional to film thickness). However, this temperature dependent behavior seemed reversible. When temperature getting back to room temperature ( $20^\circ\text{C}$ ), the capacitance curve showed little deviation from the original one.

#### 2.4. Sensing mechanism and spatial resolution

The ultra-high sensitivity of the GO foam pressure sensor is ascribed to the structure of the GO foam and its high relative dielectric permittivity. The as-prepared GO foam acted like a

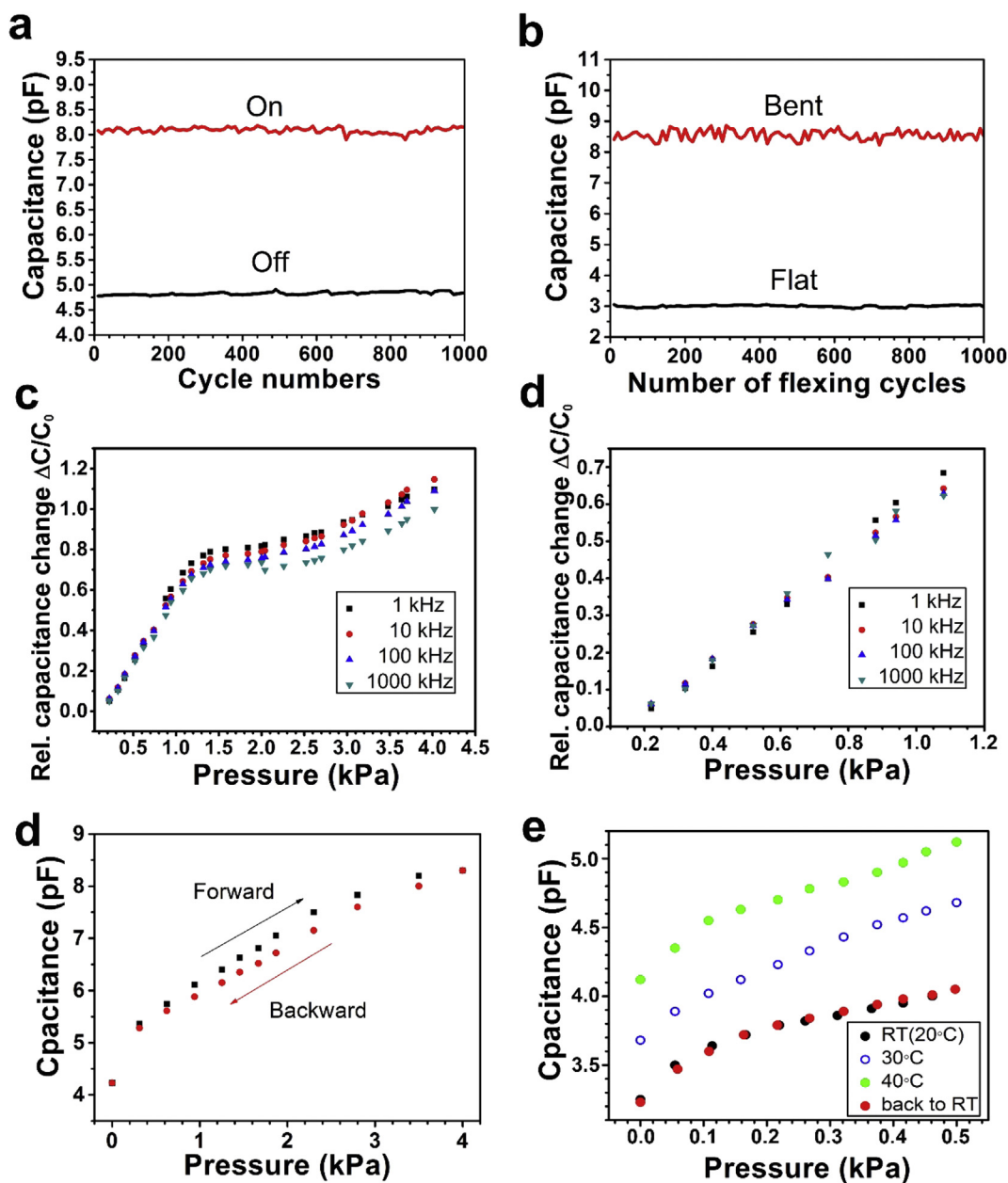


**Fig. 3.** Stability of the GO pressure sensor. (a) Capacitance of the GO foam pressure sensor in 1000 cycles of loading–unloading. (b) Capacitance of the GO foam pressure sensor over 1000 bending cycles. (c) Capacitive response to pressure at frequencies of 1, 10, 100, and 1000 kHz. All the four curves exhibit almost the same variation tendency. (d) The low pressure regime in (c) and all four near-linear curves show almost the same slope ( $\sim 0.8\text{ kPa}^{-1}$ ). (e) Pressure hysteresis of the sensor. (f) Temperature dependence of the sensor. (A colour version of this figure can be viewed online.)

sponge. The density of this GO foam was only  $4.8 \text{ mg cm}^{-3}$ ; it was light enough and could be placed onto the stamen of a flower without causing any damages (supporting information Fig. S8). This condition means that this monolith is a mixture of GO skeleton and air. According to the SEM image shown in Fig. 1 (d), a well-ordered porous 3D network consisting of 2D sheets was created. These GO sheets that are very thin (high magnification SEM image in supporting information Fig. S9) are highly interconnected through plenty of junctions; such an interconnection possibly attributes to the novel mechanical properties of the GO foam. The porous

structure provides voids which allow the GO foam to elastically deform upon the applied external pressure. The structure transformation of the GO foams by a loading–unloading cycle is schematically shown in Fig. 4 (a). By applying external pressure, the GO foams were compressed, resulting in air displacement. Therefore, the increase in capacitance in the GO foams is ascribed to the effective dielectric constant increase along with the distance reduction between the two electrode plates. The structure difference between the original GO foam and the one under pressure determined through scanning electron microscopy is clearly shown

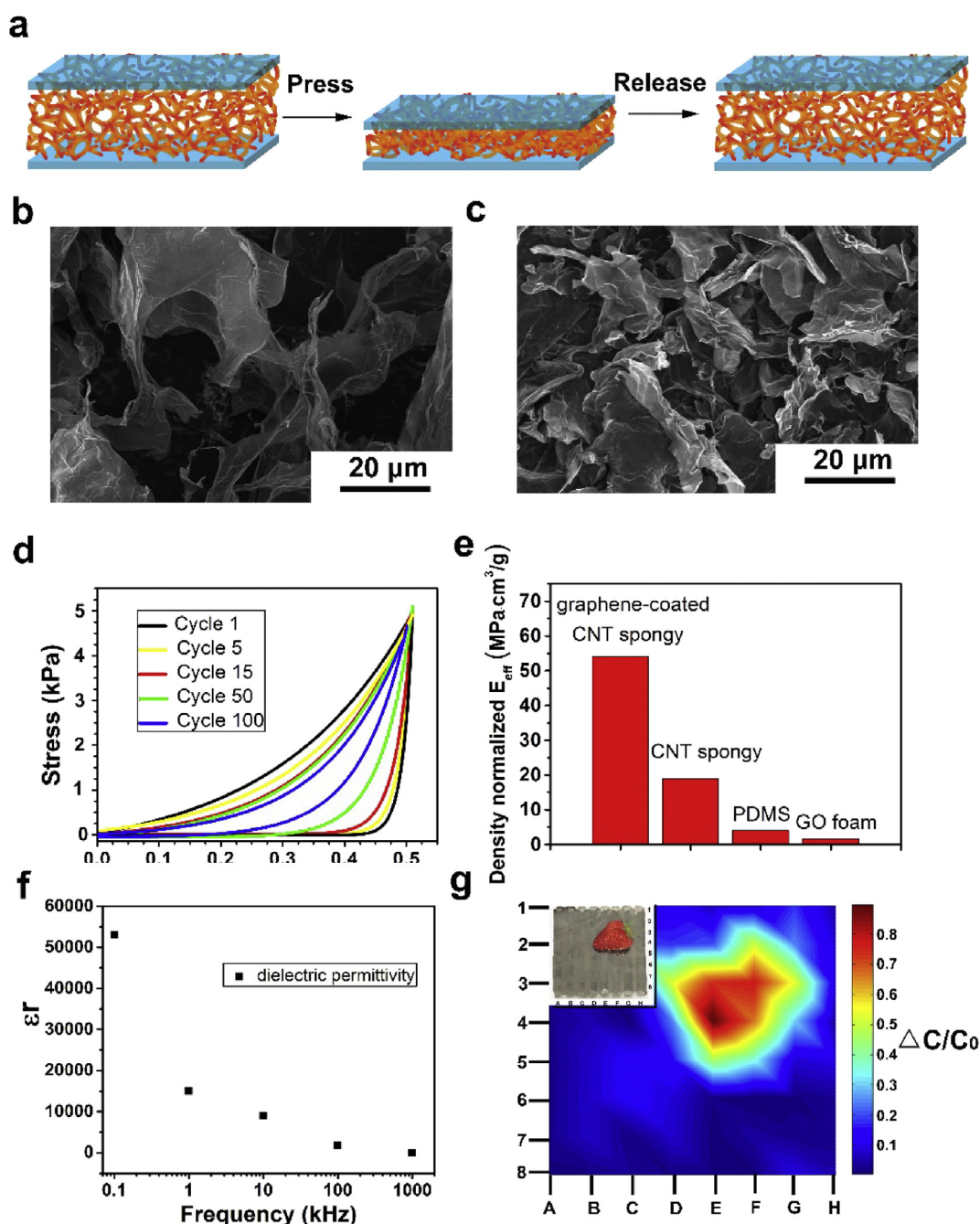


**Fig. 4.** Elasticity of the GO foam and spatial resolution of pressure sensor arrays. (a) Schematic of the loading–unloading cycle for the GO foam pressure sensor. (b) and (c) are SEM images of the original GO foam and GO foam under pressure, respectively. (d) 100 consecutive compression tests on the GO foam. (e) Comparison to low-modulus elastomer and foams, GO foam shows lower normalized  $E_{\text{eff}}$ , which means it is easier to be compressed by the same external load. (f) Relative dielectric permittivity measurement at different frequency. (g) These pressure-sensor arrays were built with thin GO foam sandwiched between reduced GO electrode-containing PET sheets with a standing strawberry (~18 g) and the pressure response to the strawberry. Insert: Bird's eye view of the strawberry standing on the sensor arrays. (A colour version of this figure can be viewed online.)

in Fig. 4 (b) and 4 (c). The GO sheets became denser under external pressure. Fig. 4 (d) shows a plot of strain versus stress for 100 loading cycles of a GO foam sample (height:  $\sim 0.8$  cm; area:  $7.1$  cm<sup>2</sup>). In the loading cycles, the maximum stress and strain values were about 5 kPa and 50%, respectively. According to a previous study [14], effective elastic modulus ( $E_{\text{eff}}$ ) is defined as the slope of the applied stress versus strain and can describe the elasticity of GO foam. The GO foam in the current study exhibited a very low  $E_{\text{eff}}$  at low pressure regime; the low value increased with compression.  $E_{\text{eff}}$  at 1 kPa was 8.2 kPa, which is much smaller than that of polydimethylsiloxane (PDMS) [56], which is a typical low-modulus elastomer.  $E_{\text{eff}}$  normalized by density was calculated to be  $\sim 1.71$  MPa cm<sup>3</sup> g<sup>-1</sup>, which is also lower than the modulus values of many polymers [57] and carbon nanotubes [58,59] based foams. By compared to low-modulus elastomer and foams shown in Fig. 4 (e), GO foam shows lower normalized  $E_{\text{eff}}$ , which means it's easier to be compressed by the same external load for GO foam. Slight plastic deformation appeared in the first cycle of compression shown in Fig. 4 (d), whereas that in subsequent cycles was effectively indistinguishable. Compared with original GO foam, microstructure damage happened after 100 loading-unloading cycles, which was certified by the SEM images in Fig. S6 (a) and (c) (supporting information). The GO foam will remain stable and porous until the pressure reaching 20 kPa, under which the GO foam was pressed to a flat membrane. What's more, the relative dielectric permittivity result is shown in Fig. 4 (f), which is similar to Liu's [51] and exhibits a high relative dielectric permittivity.

Owing to the good elasticity and high relative dielectric permittivity, a prototype capacitive pressure sensor array with 64 pixels sandwiched between reduced GO electrode-containing PET sheets was fabricated to collect spatially resolved pressure information, which is highly desirable in realizing human-computer interface applications. Each of the pixels measured  $\sim 64$  mm<sup>2</sup> ( $8 \times 8$  mm<sup>2</sup>), and the spacing between electrodes was 8 mm. The weight distribution can be recorded on each pixel by measuring the pixel capacitance. The patterned reduced GO line electrodes can be used as address and data lines. Fig. 4 (g) show the response of the sensor array to the placement of a strawberry ( $\sim 18$  g, the corresponding pressure is  $\sim 3$  kPa for one sensor). Darker color areas correspond to higher capacitances, and the darker areas with greater compression in correspond properly to the location where the strawberry stands. Points E3, E4, F3 and F4 are the darkest in the heat map in Fig. 4(g), which reflects the exact place where the strawberry was placed shown in the inset photograph. The prototype sensor array has enough spatial resolution to locate the pressure distribution and demonstrates a potential for use in pressure-sensing devices in human-computer interface applications.

A new concept application was implemented to impart pressure detection to GO by forming a porous foam-like structure. In previous reports [52,53], GO foam was usually applied in energy storage, environmental protection, and so on. In this study, we prepared thin GO foam as a compressible dielectric layer through a novel multiphase synthesis strategy to fabricate a capacitive pressure sensor with many good properties, indicating that GO foam is a candidate for flexible pressure sensing. Both elastic property and high relative dielectric permittivity make GO foam pressure sensors surpass most previously developed capacitive pressure sensors and become one of the most sensitive capacitive sensors. In addition, the overall comparison for densities, moduli, sensitivities, limits of detection of the different sensors has been summarized in Table S1 in supporting information. Fig. 5 is the radar chart to show a comparison of the sensing characteristics of typical capacitive pressure sensors. Base-signal-normalized sensitivity  $S$  of the lightest GO foam is  $2 \times 10^3$  times higher than that of a flat PDMS

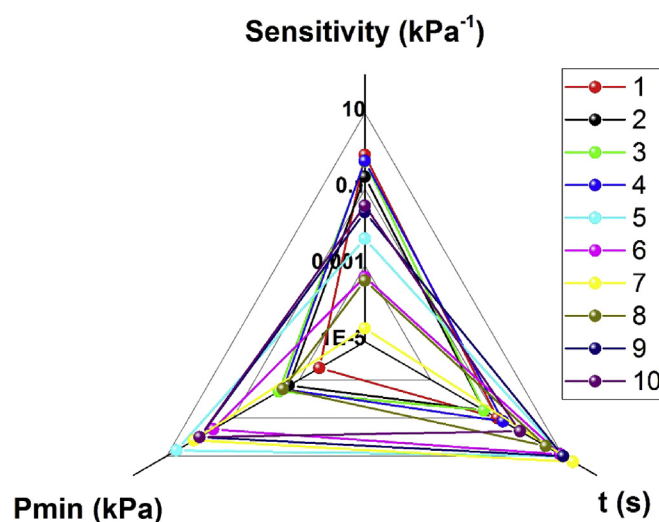


Fig. 5. Comparison of three key parameters (sensitivity, response time and pressure detecting limit) associated with capacitive pressure sensors. In the radar chart, 1 (Red) is our result, compared with 2 (Black, PDMS-coated layer, Ref. [40]), 3 (Green, fluorosilicone, Ref. [44]), 4 (Blue, structured PDMS, Ref. [6]), 5 (Cyan, air, Ref. [39]), 6 (Magenta, polyolefin foam, Ref. [38]), 7 (Yellow, flat PDMS, Ref. [37]), 8 (Dark yellow, PDMS bump, Ref. [43]), 9 (Navy, polyester pile, Ref. [42]) and 10 (Purple, cytop, Ref. [41]). (A colour version of this figure can be viewed online.)

layer [37],  $1.6 \times 10^3$  times higher than that of polyolefin foam [38],  $1.6 \times 10^2$  times higher than that of air gap [39], 4 times higher than that of a PDMS-coated layer [40], and higher than the sensitivity of a structured PDMS layer ( $0.55$  kPa<sup>-1</sup>) [6]. This GO-based capacitive pressure sensor had the ability to sense the placement and removal of a small flower petal with a pressure of 0.24 Pa. To our knowledge, this is the first flexible capacitive pressure sensor which can detect such low pressure.

### 3. Conclusion

In summary, GO foam was designed into a dielectric layer composed of porous microstructures, endowed with structure-derived elasticity. This elasticity together with high relative dielectric permittivity enables reasonable designs for high sensitivity, rapid response, and stable capacitive pressure sensors. Combining the structure-derived elasticity with high relative dielectric permittivity of the GO foam, our capacitive pressure sensor presents unprecedented sensitivity. The GO foam capacitive pressure sensors, with the good properties of high sensitivity, good reproducibility, and rapid response time, exhibit a great application potential in various fields, especially for the areas needing subtle pressure detecting in the low loading range, including flexible human-computer interfaces and robotics. For instance, this sensor can be integrated into car's steering wheel to monitor the conditions of the driver. If the tired driver has the trend to loose the steering wheel, sensors will detect the subtle pressure change and then warn the driver. This research also predicts that GO foam will be highly useful in flexible devices because of its advantageous traits, including structural controllability, good elasticity, and high relative dielectric permittivity.

### Acknowledgements

This work was supported by the National Natural Science Foundation of China (Nos 11525415, 51302037, 61274114, 51420105003, 11327901 and 11204034).

## Appendix A. Supplementary data

Supplementary data related to this article can be found at <http://dx.doi.org/10.1016/j.carbon.2016.12.023>.

## References

- [1] D. Kinwande, N. Petrone, J. Hone, Two-dimensional flexible nanoelectronics, *Nat. Commun.* 5 (2014) 5678–5679.
- [2] X. Huang, Y. Liu, H. Cheng, W.J. Shin, J.A. Fan, Z. Liu, C.J. Lu, G.W. Kong, K. Chen, D. Patnaik, S.H. Lee, S. Hage-Ali, Y. Huang, J.A. Rogers, Materials and designs for wireless epidermal sensors of hydration and strain, *Adv. Funct. Mater.* 24 (2014) 3846–3854.
- [3] W. Zeng, L. Shu, Q. Li, S. Chen, F. Wang, X.M. Tao, Fiber-based wearable electronics: a review of materials, fabrication, devices, and applications, *Adv. Mater.* 26 (31) (2014) 5310–5336.
- [4] D.H. Kim, N.S. Lu, R. Ma, Y.S. Kim, R.H. Kim, S.D. Wang, J. Wu, S.M. Won, H. Tao, A. Islam, K.J. Yu, T. Kim, R. Chowdhury, M. Ying, L.Z. Xu, M. Li, H.J. Chung, H. Keum, M. McCormick, P. Liu, Y.W. Zhang, F.G. Omenetto, Y.G. Huang, T. Coleman, J.A. Rogers, Epidermal electronics, *Science* 333 (6044) (2011) 838–843.
- [5] M.L. Hammock, A. Chortos, B.C.K. Tee, J.B.H. Tok, Z. Bao, 25th Anniversary Article: the evolution of electronic skin (E-Skin): a brief history, design considerations, and recent progress, *Adv. Mater.* 25 (42) (2013) 5997–6038.
- [6] S.C.B. Mannsfeld, B.C.K. Tee, R.M. Stoltenberg, C.V.H.H. Chen, S. Barman, B.V.O. Muir, A.N. Sokolov, C. Reese, Z. Bao, Highly sensitive flexible pressure sensors with microstructured rubber dielectric layers, *Nat. Mater.* 9 (10) (2010) 859–864.
- [7] T.T. Tung, C. Robert, M. Castro, J.F. Feller, T.Y. Kim, K.S. Suh, Enhancing the sensitivity of graphene/polyurethane nanocomposite flexible piezo-resistive pressure sensors with magnetite nano-spacers, *Carbon* 108 (2016) 450–460.
- [8] K. Takei, T. Takahashi, J.C. Ho, H. Ko, A.G. Gillies, P.W. Leu, R.S. Fearing, A. Javey, Nanowire active-matrix circuitry for low-voltage macroscale artificial skin, *Nat. Mater.* 9 (2010) 821–826.
- [9] S. Chun, Y. Kim, H. Jin, E. Choi, S.B. Lee, W. Park, A graphene force sensor with pressure-amplifying structure, *Carbon* 78 (2014) 601–608.
- [10] G. Schwartz, B.C.K. Tee, J. Mei, A.L. Appleton, D.H. Kim, H. Wang, Z. Bao, Flexible polymer transistors with high pressure sensitivity for application in electronic skin and health monitoring, *Nat. Commun.* 4 (2013) 1859–1866.
- [11] M. Habibi, S. Darbari, S. Rajabali, V. Ahmadi, Fabrication of a graphene-based pressure sensor by utilizing field emission behavior of carbon nanotubes, *Carbon* 96 (2016) 259–267.
- [12] W.L. Hu, X.F. Niu, R. Zhao, Q.B. Pei, Elastomeric transparent capacitive sensors based on an interpenetrating composite of silver nanowires and polyurethane, *Appl. Phys. Lett.* 102 (2013) 083303.
- [13] J. Hwang, J. Jang, K. Hong, K.N. Kim, J.H. Han, K. Shin, C.E. Park, Poly(3-hexylthiophene) wrapped carbon nanotube/poly(dimethylsiloxane) composites for use in finger-sensing piezoresistive pressure sensors, *Carbon* 49 (2011) 106–110.
- [14] L. Pan, A. Chortos, G. Yu, Y. Wang, S. Isaacson, R. Allen, Y. Shi, R. Dauskardt, Z. Bao, An ultra-sensitive resistive pressure sensor based on hollow-sphere microstructure induced elasticity in conducting polymer film, *Nat. Commun.* 5 (2014) 3002–3009.
- [15] F. Michelis, L. Bodelot, Y. Bonnassieux, B. Lebental, Highly reproducible, hysteresis-free, flexible strain sensors by inkjet printing of carbon nanotubes, *Carbon* 95 (2015) 1020–1026.
- [16] Y.J. Yang, M.Y. Cheng, W.Y. Chang, L.C. Tsao, S.A. Yang, W.P. Shih, F.Y. Chang, S.H. Chang, K.C. Fan, An integrated flexible temperature and tactile sensing array using PI-copper films, *Sensors Actuators A Phys.* 143 (2008) 143–153. <http://www.sciencedirect.com/science/article/pii/S0924424707008126-v1>. <http://www.sciencedirect.com/science/article/pii/S0924424707008126-v2>. <http://www.sciencedirect.com/science/article/pii/S0924424707008126-v3>. <http://www.sciencedirect.com/science/article/pii/S0924424707008126-v4>. <http://www.sciencedirect.com/science/article/pii/S0924424707008126-v5>. <http://www.sciencedirect.com/science/article/pii/S0924424707008126-v6>. <http://www.sciencedirect.com/science/article/pii/S0924424707008126-v7>. <http://www.sciencedirect.com/science/article/pii/S0924424707008126-v8>.
- [17] J. Feng, L. Peng, C. Wu, X. Sun, S. Hu, C. Lin, J. Dai, J. Yang, Y. Xie, Giant moisture responsiveness of  $\text{V}_2\text{S}_5$  ultrathin nanosheets for novel touchless positioning interface, *Adv. Mater.* 24 (2012) 1969–1974.
- [18] T. Someya, T. Sekitani, S. Iba, Y. Kato, H. Kawaguchi, T. Sakurai, A large-area, flexible pressure sensor matrix with organic field-effect transistors for artificial skin applications, *Proc. Natl. Acad. Sci. U. S. A.* 101 (27) (2004) 9966–9970.
- [19] I. Graz, M. Kaltenbrunner, C. Keplinger, R. Schwödauier, S. Bauer, S.P. Lacour, S. Wagner, Flexible ferroelectric field-effect transistor for large-area sensor skins and microphones, *Appl. Phys. Lett.* 89 (2006) 073501.
- [20] Y. Zang, F. Zhang, D. Huang, X. Gao, C. Di, D. Zhu, Flexible suspended gate organic thin-film transistors for ultra-sensitive pressure detection, *Nat. Commun.* 6 (2015) 6269–6277.
- [21] C. Pang, G.Y. Lee, T. Kim, S.M. Kim, H.N. Kim, S.H. Ahn, K.Y. Suh, A flexible and highly sensitive strain-gauge sensor using reversible interlocking of nanofibres, *Nat. Mater.* 11 (2012) 795–801.
- [22] M. Shimojo, A. Namiki, M. Ishikawa, R. Makino, K. Mabuchi, A tactile sensor sheet using pressure conductive rubber with electrical-wires stitched method, *IEEE Sensors J.* 4 (5) (2004) 589–596.
- [23] C.L. Choong, M.B. Shim, B.S. Lee, S. Jeon, D.S. Ko, T.H. Kang, J. Bae, S.H. Lee, K.E. Byun, J. Im, Y.J. Jeong, C.E. Park, J.J. Park, U. Chung, Highly stretchable resistive pressure sensors using a conductive elastomeric composite on a micropylamid array, *Adv. Mater.* 26 (21) (2014) 3451–3458.
- [24] S. Gong, W. Schwab, Y. Wang, Y. Chen, Y. Tang, J. Si, B. Shirinzadeh, W. Cheng, A wearable and highly sensitive pressure sensor with ultrathin gold nanowires, *Nat. Commun.* 5 (2013) 3132–3139.
- [25] F. Michelis, L. Bodelot, Y. Bonnassieux, B. Lebental, Highly reproducible, hysteresis-free, flexible strain sensors by inkjet printing of carbon nanotubes, *Carbon* 95 (2015) 1020–1026.
- [26] S. Chun, H. Jung, Y. Choi, G. Bae, J.P. Kil, W. Park, A tactile sensor using a graphene film formed by the reduced graphene oxide flakes and its detection of surface morphology, *Carbon* 94 (2015) 982–987.
- [27] S.J. Park, D.W. Kim, S.W. Jang, M.L. Jin, S.J. Kim, J.M. Ok, J.S. Kim, H.T. Jung, Fabrication of graphite grids via stencil lithography for highly sensitive motion sensors, *Carbon* 96 (2016) 491–496.
- [28] H.B. Yao, J. Ge, C.F. Wang, X. Wang, W. Hu, Z.J. Zheng, Y. Ni, S.H. Yu, A flexible and highly pressure-sensitive graphene-polyurethane sponge based on fractured microstructure design, *Adv. Mater.* 25 (46) (2013) 6692–6698.
- [29] M. Ha, S. Lim, J. Park, D.S. Um, Y. Lee, H. Ko, Electronic skin: bioinspired interlocked and hierarchical design of ZnO nanowire arrays for static and dynamic pressure-sensitive electronic skins, *Adv. Funct. Mater.* 25 (19) (2015) 2841–2849.
- [30] M. Segev-Bar, H. Haick, Flexible sensors based on nanoparticles, *ACS Nano* 7 (10) (2013) 8366–8378.
- [31] M. Segev-Bar, G. Konvalina, H. Haick, Resolution unpixelated electronic skin strip with anti-parallel thickness gradients of nanoparticles, *Adv. Mater.* 27 (10) (2015) 1779–1784.
- [32] B.C.K. Tee, C. Wang, R. Allen, Z. Bao, An electrically and mechanically self-healing composite with pressure- and flexion-sensitive properties for electronic skin applications, *Nat. Nanotechnol.* 7 (2012) 825–832.
- [33] T.P. Huynh, H. Haick, Self-healing, fully functional, and multiparametric flexible sensing platform, *Adv. Mater.* 28 (1) (2016) 138–143.
- [34] B. Zhu, H. Wang, Y. Liu, D. Qi, Z. Liu, H. Wang, J. Yu, M. Sherburne, Z. Wang, X. Chen, Skin-inspired haptic memory arrays with an electrically reconfigurable architecture, *Adv. Mater.* 28 (8) (2016) 1559–1566.
- [35] F. Fan, L. Lin, G. Zhu, W. Wu, R. Zhang, Z. Wang, Transparent triboelectric nanogenerators and self-powered pressure sensors based on micropatterned plastic films, *Nano Lett.* 12 (6) (2012) 3109–3114.
- [36] L.Y. Chen, B.C.K. Tee, A.L. Chortos, G. Schwartz, V. Tse, D.J. Lipomi, H.S.P. Wong, M.V. McConnell, Z. Bao, Continuous wireless pressure monitoring and mapping with ultra-small passive sensors for health monitoring and critical care, *Nat. Commun.* 5 (2014) 5028–5037.
- [37] B. Zhang, Z. Xiang, S. Zhu, Q. Hu, Y. Cao, J. Zhong, Q. Zhong, B. Wang, Y. Fang, B. Hu, J. Zhou, Z.L. Wang, Dual functional transparent film for proximity and pressure sensing, *Nano Res.* 7 (10) (2014) 1488–1496.
- [38] C. Metzger, E. Fleisch, J. Meyer, M. Danschmüller, I. Graz, M. Kaltenbrunner, C. Keplinger, R. Schwödauier, S. Bauer, Flexible-foam-based capacitive sensor arrays for object detection at low cost, *Appl. Phys. Lett.* 92 (2008) 013506.
- [39] H.K. Lee, S.I. Chang, E. Yoon, A flexible polymer tactile sensor: fabrication and modular expandability for large area deployment, *J. Microelectromech. Syst.* 15 (6) (2006) 1681–1686.
- [40] J. Lee, H. Kwon, J. Seo, S. Shin, J.H. Koo, C. Pang, S. Son, J.H. Kim, Y.H. Jang, D.E. Kim, T. Lee, Sensors: conductive fiber-based ultrasensitive textile pressure sensor for wearable electronics, *Adv. Mater.* 27 (15) (2015) 2433–2439.
- [41] S. Takamatsu, T. Kobayashi, N. Shibayama, K. Miyake, T. Itoh, Fabric pressure sensor array fabricated with die-coating and weaving techniques, *Sensors Actuators A Phys.* 184 (2012) 57–63.
- [42] J. Meyer, B. Arnrich, J. Schumm, G. Tröster, Design and modeling of a textile pressure sensor for sitting posture classification, *IEEE Sensors J.* 10 (8) (2010) 1391–1398.
- [43] F.K. Lei, K.F. Lee, M.Y. Lee, A flexible PDMS capacitive tactile sensor with adjustable measurement range for plantar pressure measurement, *Microsyst. Technol.* 20 (7) (2014) 1351–1358.
- [44] L. Viry, A. Levi, M. Totaro, A. Mondini, V. Mattoli, B. Mazzolai, L. Beccai, Flexible three-axial force sensor for soft and highly sensitive artificial touch, *Adv. Mater.* 26 (17) (2014) 2659–2664.
- [45] K.S. Novoselov, A.K. Geim, S.V. Morozov, D. Jiang, Y. Zhang, S.V. Dubonos, I.V. Grigorieva, A.A. Firsov, Electric field effect in atomically thin carbon films, *Science* 306 (5696) (2004) 666–669.
- [46] A.K. Geim, K.S. Novoselov, The rise of graphene, *Nat. Mater.* 6 (3) (2007) 183–191.
- [47] S.J. Park, R.S. Ruoff, Chemical methods for the production of graphenes, *Nat. Nanotechnol.* 4 (2009) 217–224.
- [48] A. Lerf, H. He, M. Förster, J. Klinowski, Structure of graphite oxide revisited, *J. Phys. Chem. B* 102 (23) (1998) 4477–4482.
- [49] W. Cai, R.D. Piner, F.J. Stadermann, S.M. Park, A. Shaibat, Y. Ishii, D. Yang, A. Velamakanni, S.J. An, M. Stoller, J. An, D. Chen, R.S. Ruoff, Synthesis and solid-state NMR structural characterization of  $^{13}\text{C}$ -labeled graphite oxide, *Science* 321 (5897) (2008) 1815–1817.
- [50] C. Gómez-Navarro, R.T. Weitz, A.M. Bittner, M. Scolari, A. Mews, M. Burghard, K. Kern, Electronic transport properties of individual chemically reduced

- graphene oxide sheets, *Nano Lett.* 7 (11) (2007) 3499–3503.
- [51] J. Liu, D. Galpaya, M. Notarianni, C. Yan, N. Motta, Graphene-based thin film supercapacitor with graphene oxide as dielectric spacer, *Appl. Phys. Lett.* 103 (2013) 063108.
- [52] H. Bi, X. Xie, K. Yin, Y. Zhou, S. Wan, L. He, F. Xu, F. Banhart, L. Sun, R.S. Ruoff, Spongy graphene as a highly efficient and recyclable sorbent for oils and organic solvents, *Adv. Funct. Mater.* 22 (21) (2012) 4421–4425.
- [53] H. Bi, X. Xie, K. Yin, Y. Zhou, S. Wan, R.S. Ruoff, L. Sun, Highly enhanced performance of spongy graphene as oil sorbent, *J. Mater. Chem. A* 2 (6) (2014) 1652–1656.
- [54] X. Wang, L.L. Lu, Z.L. Yu, X.W. Xu, Y.R. Zheng, S.H. Yu, Scalable template synthesis of resorcinol-formaldehyde/graphene oxide composite aerogels with tunable densities and mechanical properties, *Angew. Chem.* 54 (8) (2015) 2397–2401.
- [55] H. Sun, Z. Xu, C. Gao, Multifunctional, ultra-flyweight, synergistically assembled carbon aerogels, *Adv. Mater.* 25 (18) (2013) 2554–2560.
- [56] J. Mark, *Polymer Data Handbook*, 2nd ed., Oxford Univ. Press, 1999.
- [57] L.J. Gibson, M.F. Ashby, *Cellular Solids: Structure and Properties*, Cambridge Univ. Press, 1997.
- [58] K.H. Kim, Y. Oh, M.F. Islam, Graphene coating makes carbon nanotube aerogels superelastic and resistant to fatigue, *Nat. Nanotechnol.* 7 (2012) 562–566.
- [59] X. Gui, J. Wei, K. Wang, A. Cao, H. Zhu, Y. Jia, Q. Shu, D. Wu, Carbon nanotube sponges, *Adv. Mater.* 22 (5) (2010) 617–621.